Low-loss all-solid photonic bandgap fiber

Guobin Ren, Ping Shum, Liren Zhang, and Xia Yu

Network Technology Research Centre, Nanyang Technological University, 50 Nanyang Drive, Singapore 637553

Weijun Tong and Jie Luo

Yangtze Optical Fiber and Cable Company Ltd., Guanshan 2 Road, Wuhan, China 430073

Received December 5, 2006; revised January 12, 2007; accepted January 26, 2007;
posted February 1, 2007 (Doc. ID 77792); published April 3, 2007

We report the fabrication and characterization of a new type all-solid photonic bandgap fiber. By introducing an index depressed layer around the high-index rod in the unit cell of photonic crystal cladding, transmission loss as low as 2 dB/km within the first bandgap is realized for the all-solid photonic bandgap fiber with a bandwidth of over 700 nm. The bend loss experiment shows that the photonic bandgap fiber is much less bend sensitive than single-mode fiber. © 2007 Optical Society of America

OCIS codes: 060.2310, 060.2280, 060.2270.

The all-solid photonic bandgap fiber (PBGF) is an optical fiber in which the cladding comprises an arrangement of isolated high-index rods in low-index background.[1–3] The antiresonant reflection optical waveguide model[4,5] has been successfully applied to understand the guidance mechanism of the all-solid PBGF. All-solid PBGFs provide a promising technology to fabricate bandgap materials with the usual process used in conventional fiber drawing. Compared with the air-core bandgap fiber, the all-solid PBGF is better able to realize a rare-earth-doped amplifier and laser or to write Bragg gratings that are widely used in photonics. Moreover these fibers should be easier to fabricate and splice for the PBGF's elimination of mechanically unstable holey structure. At present, the lowest loss for such all-solid PBGFs is $\sim$20/dB km.[6] But almost all these fibers utilize the high-order bandgaps.[6–8] Although high-order bandgaps provide lower confinement loss, they are more sensitive to fiber deformation, and the photonic bands of high-order rod modes will greatly narrow the transmission windows of the fiber. Moreover, these fibers have been found to suffer from significant bend loss under certain circumstances. Generally speaking, seven to eight rings of high-index rods are required for reduction of the confinement loss; and working in higher bandgaps at a fixed wavelength would require larger pitch, which will result in thicker fibers.

It has been shown[9] that, by introducing an index-depressed layer around the high-index rods in fiber cladding, the confinement and bend losses of the PBGF would be greatly improved compared with the all-solid PBGF, whose cladding consists of simple high-index rods, especially in low-order (first and second) bandgaps. In this Letter, we report the fabrication and characterization of such a new type of PBGF. The fiber has shown attenuation as low as 2 dB/km, with a bandwidth of over 700 nm. The bend-loss experiment shows that the PBGF is much less bend sensitive than a step-index single-mode fiber (SISMF).

A doped silica preform is used to build the periodic structure of the cladding. The refractive index profile of the preform is shown in Fig. 1(a). The preform is composed of a central high-index part (germanium doped) with a quasi-parabolic index profile surrounded by an index depressed layer (fluorine doped); the doped part is overcladded with a pure silica jacket. The maximum refractive index differences of the germanium-doped and fluorine-doped area are approximately $3.67.10^{-2}$ and $-8.4.10^{-3}$, compared with the pure silica background. The outer diameter of the preform is etched to 14.5 mm. We then draw the preform to canes to stack them in a hexagonal pattern. The core is formed by replacing the central doped silica cane with a pure silica one. The stack is then jacketed and drawn to form PBGF, which is shown in Fig. 1(b). The inset of Fig. 1(b) shows the scanning electron micrograph (SEM) of the fiber cross section close to the core. The fiber is coated with a polymer during the draw.

The diameter of the fiber is 175 μm; the lattice spacing Λ is $\sim$7.23 μm. The relative diameters of the high- and low-index layer in the unit cell of the cladding are $d_h/\Lambda = 0.42$ and $d_l/\Lambda = 0.75$, respectively. The sizes of the high- and low-index layer cannot be determined accurately according to the SEM picture, we assume that the refractive index profile has not

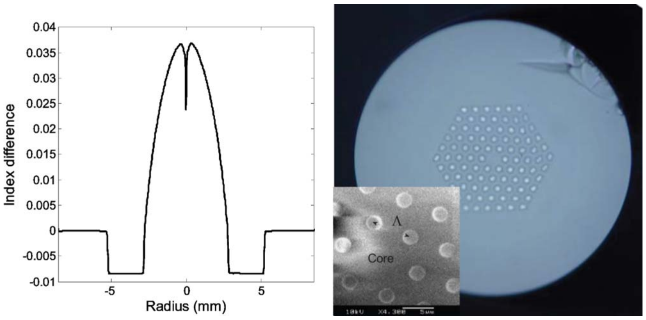

Fig. 1. (Color online) (a) Refractive index profile of doped silica preform used to build the periodic structure of fiber cladding. (b) Optical micrograph of the fabricated PBGF. High- and low-index regions appear lighter and darker, respectively, in the image. The outer diameter of the fiber is 175 μm. The inset shows the SEM of the fiber cross section close to the core. Only the germanium-doped part can be identified within each periodic cell.

0146-9592/07/091023-3/$15.00

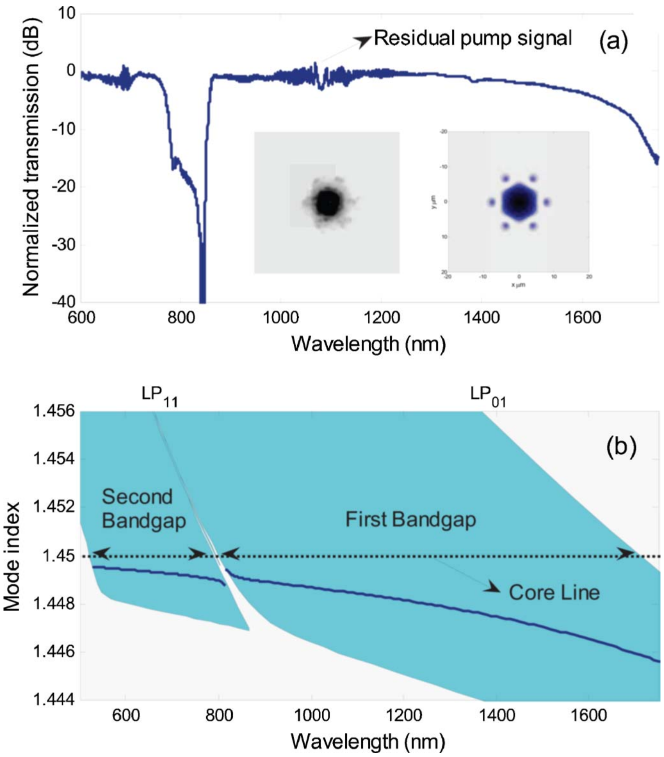

Fig. 2. (Color online) (a) Normalized transmission spectrum of 5 m PBGF. (b) Bandgap and guided modes of the PBGF. (a) Left inset, output near-field image from 2 m of fiber at 1550 nm wavelength. (a) Right inset, the calculated intensity profile at the same wavelength.

been significantly modified during the drawing process.

The spectral transmission through the all-solid PBGF is measured by using a photonic-crystal-fiber-based broadband supercontinuum source. Since the core diameter of the PBGF is ~9 μm, it is comparable with a standard SMF. The broadband supercontinuum source is coupled into a SMF, and the output is butted against one end of the PBGF. We then adjust the alignment to maximize the power in the core at the other end of the PBGF. The transmitted spectrum is measured by using an optical spectrum analyzer (OSA). Figure 2(a) shows the normalized transmission spectrum (normalized to output of the SMF) of 5 m PBGF. The wavelength span is 600–1750 nm, which is limited by the detection bandwidth of the OSA. The bandgap map and guided core mode of the PBGF are shown in Fig. 2(b). The photonic bands formed by the coupling of the modes of isolated high-index rods are marked at the top of the map. The core line $n_{eff}=1.45$ represents the boundary between states that are propagating or evanescent in background material of cladding. It can be seen that the first and second bandgaps are located at 820–1720 and 530–790 nm, respectively, which correspond to the low-loss transmission windows shown in Fig. 2(a). It is noted that the low-order bandgaps are much wider and more deformation resistant than high-order ones,[3] therefore it is desirable to operate a fiber in the first bandgap.

The modal profile of the fiber has been measured by injecting the light from a tunable laser into the PBGF, and the fiber output end is imaged on an infrared CCD camera. The intensity profile observed for a fiber length of 2 m at 1550 nm wavelength is shown in the left inset of Fig. 2(a). No other core modes or rod modes are observed when we vary the injection conditions or bend (twist) the fiber. The mode is mainly confined in the core region with six satellite spots around the fiber core. The right inset of Fig. 2(a) shows the computed intensity of modal field of the fiber, which agrees with the experimental result shown in the left.

The attenuation spectrum of the 490 m long PBGF has been measured by the cut-back technique and plotted in Fig. 3. Broadband transmission has been observed from 880 to 1600 nm, which corresponds to the first bandgap. The bandwidth is over 700 nm, this wideband operation is enabled by using the first bandgap. The minimal loss (~2 dB/km) occurs at a wavelength of 1310 nm. To the best of our knowledge, this is the best result ever reported for all-solid PBGFs.[8] At 1490 and 1550 nm, the attenuation is 5.9 and 13 dB/km, respectively. It is possible to shift the minimal attenuation to ~1550 nm by scaling the fiber diameter or lattice spacing.

It is noticed that only five rings of the high-index rods are included in our fiber cladding, compared with seven to eight rings required for previous all-solid PBGFs. The diameter of the fiber is 175 μm, it is possible to reduce it to 125 μm by selecting a thinner jacket tube during the preform fabrication process. The high attenuation peak at ~1380 nm and the peaks at 950 and 1240 nm are OH^- absorption (see Fig. 3). It is believed that our experimental level of loss is limited by water contamination during the stacking process. This level can probably be reduced further by using an adequate cleaning process. Nevertheless, this level of loss is already adequately low to realize a lot of practical experiments such as Bragg gratings inscription, actively doped PBGFs, etc.

We investigated the effect of bend radius on bend loss by measuring the transmission spectrum of a 10 m PBGF with different bend radii. The transmission spectra of a PBGF with different bend radii for ten turns are shown in Fig. 4. The "straight fiber" represents a fiber with a bend radius of 15 cm, at this scale no variation of the spectral transmission with

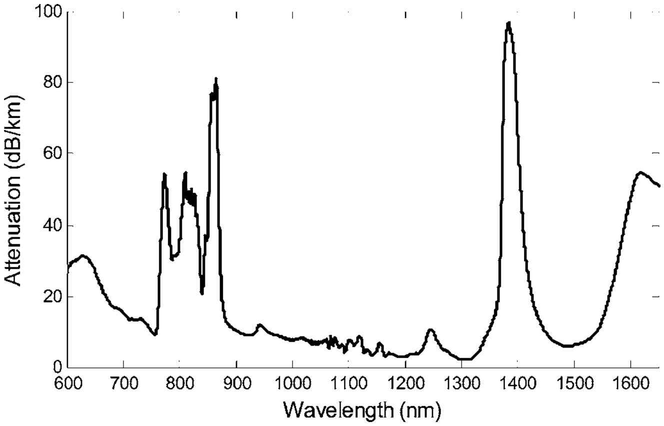

Fig. 3. Attenuation spectrum of all-solid PBGF.

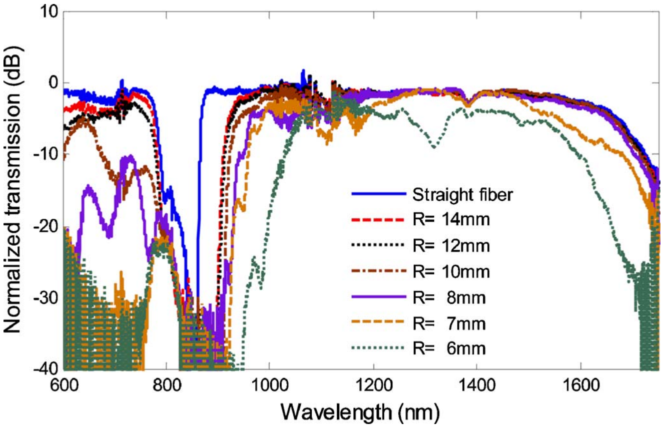

Fig. 4. (Color online) Normalized transmission spectra of the PBGF with different bend radii ($R=14$, 12, 10, 8, 7, and 6 mm) for the length of ten turns. The spectral transmission of a straight fiber is also shown.

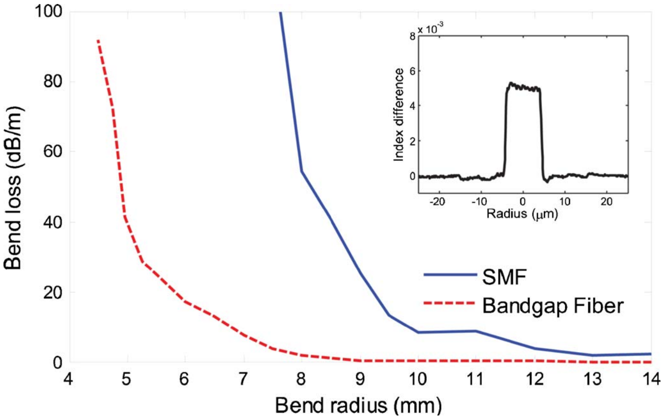

Fig. 5. (Color online) Measured bend losses for the SISMF and all-solid PBGF at a 1550 nm wavelength. The inset shows the index profile of the SISMF.

different bend radii is observed. It is noticed that the mode guided by the second bandgap is more susceptible than that guided by the first bandgap; the reason for this observation is that the index mismatch between the core mode and the photonic bands is smaller within the second bandgap than that within the first bandgap [see Fig. 2(b)]. For wavelengths in the middle of the first bandgap, the core mode is far removed from the bands above and below and is unaffected by large-radius bends. We can see that the bandgap becomes narrower as the bend radius decreases, with loss greatly increasing at the edges. The steeper slope of the blue edge of the bandgap in Fig. 4 means that the effective index mismatch between core and photonic bands increases more rapidly at that edge [also see Fig. 2(b)], so the bandgap should narrow more rapidly at the blue edge than the red edge as the fiber is bent.

It is worth noticing that the bend loss of this PBGF has been greatly improved compared with those reported earlier.[3,6–8] The reason for this observation is that the floor of the bandgaps is efficiently deepened by introducing an index depressed layer around the high-index rods in the unit cell of photonic crystal cladding. Due to the enlarged index mismatch of the guided core mode and the edge of the bandgaps, the critical bend radius of the proposed fiber is remarkably reduced.[9] Bend loss has been measured by using a narrowband tunable laser and power meter for different bend radii at 1550 nm. For the purpose of comparison, a SISMF has also been fabricated by the modified chemical-vapor deposition process. The cutoff wavelength of the SISMF is 1319 nm, and the mode field diameter is 10.4 μm at 1550 nm. Results have been plotted in Fig. 5. The refractive index profile of the SISMF is shown as an inset. The PBGF appears to be less bend-sensitive than the SISMF. For instance, for a bend radius equal to 8 mm, bend loss has been measured to be 1.8 dB/m for the PBGF, and 54.3 dB/m for the SISMF.

In our previous work,[9] by designing the profile of a unit cell in photonic crystal cladding, we theoretically predicted that the all-solid PBGF has superior performance in confinement loss and bend loss. In this Letter, we report the fabrication and characterization of this new type of all-solid PBGF. The low-loss transmission has been realized within the first bandgap. The minimal loss (~2 dB/km) occurs at a wavelength of 1310 nm. To the best of our knowledge, this is the best result ever reported for all-solid PBGFs. Since the first bandgap is utilized to guide the mode, the fiber has shown a wide transmission range from 880 to 1600 nm. Moreover, the PBGF has shown a much less bend sensitivity than SISMFs.

This work is partially supported by project M47040039 of the Agency for Science, Technology and Research, Singapore, and by the Open Fund of the Key Laboratory of Optical Communication and Lightwave Technologies (Beijing University of Posts and Telecommunications), Ministry of Education, China. R. Guobin's e-mail address is gbren@ntu.edu.sg.

References

1. F. Luan, A. K. George, T. D. Hedley, G. J. Pearce, D. M. Bird, J. C. Knight, and P. St. J. Russell, Opt. Lett. **29**, 2369 (2004).
2. A. Argyros, T. A. Birks, S. G. Leon-Saval, C. M. B. Cordeiro, F. Luan, and P. St. J. Russell, Opt. Express **13**, 309 (2005).
3. A. Argyros, T. A. Birks, S. G. Leon-Saval, C. M. B. Cordeiro, and P. St. J. Russell, Opt. Express **13**, 2503 (2005).
4. T. P. White, R. C. McPhedran, C. M. de Sterke, N. M. Litchinitser, and B. J. Eggleton, Opt. Lett. **27**, 1977 (2002).
5. N. M. Litchinitser, S. C. Dunn, B. Usner, B. J. Eggleton, T. P. White, R. C. McPhedran, and C. M. de Sterke, Opt. Express **11**, 1243 (2003).
6. G. Bouwmans, L. Bigot, Y. Quiquempois, F. Lopez, L. Provino, and M. Douay, Opt. Express **13**, 8452 (2005).
7. J. M. Stone, G. J. Pearce, F. Luan, T. A. Birks, J. C. Knight, A. K. George, and D. M. Bird, Opt. Express **14**, 6291 (2006).
8. T. A. Birks, F. Luan, G. J. Pearce, A. Wang, J. C. Knight, and D. M. Bird, Opt. Express **14**, 5688 (2006).
9. G. Ren, P. Shum, L. Zhang, M. Yan, X. Yu, W. Tong, and J. Luo, IEEE Photon. Technol. Lett. **18**, 2560 (2006).